Technical Annals

Vol 1, No 5 (2024)

Technical Annals

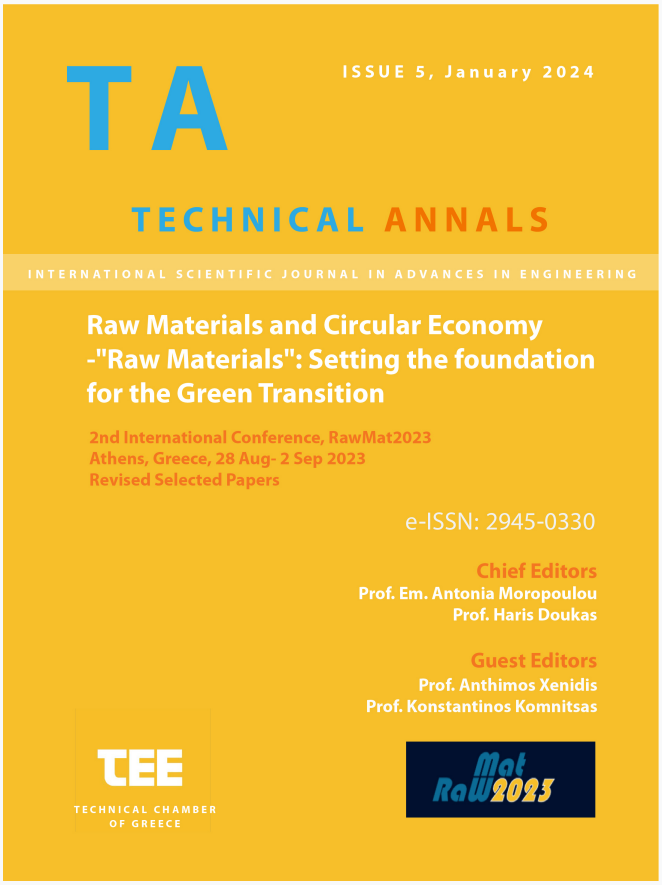

Resin-supported nanoiron: A powerful tool for heavy metal decontamination - Elucidating the mechanism through column studies

Christiana Mystrioti, Nymphodora Papassiopi, Anthimos Xenidis

doi: 10.12681/ta.37046

To cite this article:

Mystrioti, C., Papassiopi, N., & Xenidis, A. (2024). Resin-supported nanoiron: A powerful tool for heavy metal decontamination - Elucidating the mechanism through column studies. *Technical Annals*, *1*(5). https://doi.org/10.12681/ta.37046

Resin-supported nanoiron: A powerful tool for heavy metal decontamination - Elucidating the mechanism through column studies

Christiana Mystrioti[1], Nymphodora Papassiopi[1] and Anthimos Xenidis[1]

[1]Sch. of Mining and Metallurgical Eng., National Technical University of Athens, 15780, Greece
chmistrioti@metal.ntua.gr

Abstract. The significance of removing heavy metal ions from wastewater treatment plant effluents cannot be overstated in preserving a clean environment and protecting human health. Various methods, including adsorption, membrane-based processes, chemical treatments, electrical methods, and photocatalysis, have been documented for the effective removal of heavy metal ions from different wastewater sources. Nanoparticles, with their strong affinity, show promise in wastewater treatment, particularly in efficiently extracting heavy metals. This study aimed to evaluate the effectiveness of an iron nanocomposite (R-nFe), in eliminating various heavy metals from effluents of wastewater treatment plants through column tests. R-nFe is composed of nano zero valent iron (nZVI) supported in an inert cationic resin, produced using green tea extract as a reducing agent for Fe(III) to Fe(0). The introduced feed solution to the columns contained a mixture of heavy metals, including Cr(VI), As, Ni, Pb, Cu, Cd, and Zn. The study investigated the impact of contact time on the sorption and reduction rates of the selected compounds, varying contact times to 2.4, 4.8, and 6 minutes. R-nFe demonstrated high efficiency in removing Cr(VI) and As, with effluent concentrations meeting environmental limits when the contact time exceeded 5 minutes. However, the performance of R-nFe was less effective for divalent metal contaminants due to the strong competitive effect of coexisting Ca. The study provided a succinct exploration of the mechanisms involved in using the R-nFe nanocomposite for the removal of metals and metalloids.

Keywords: heavy metals, wastewater stream, water pollution, nano zero valent iron, resin, iron nanocomposite, flow conditions, removal mechanism, metal decontamination.

1 Introduction

As the global population steadily grows, the demand for freshwater resources for household, agricultural, and industrial use is on the rise [1]. Concurrently, industrial activities significantly contribute to the deterioration of water quality through the discharge of pollutants, leading to reduced availability and compromised suitability of clean water sources [2,3]. The effluents of wastewater treatment plants can be used for

various purposes, such as agriculture irrigation, landscape irrigation and industrial uses etc.

The use of treated wastewater for irrigation offers a sustainable solution, especially in regions facing water scarcity. However, the quality of the treated water is crucial, and it must meet specific standards to ensure it is safe for the intended use. Low concentrations of heavy metals and micropollutants are detected in the effluents of wastewater treatment plants (WWTPs) [4]. In a study by Du et al. (2020) [4], the concentrations of heavy metals in wastewaters were found to be Pb: 45 ± 15 μg/L; Cd: 5.2 ± 5.1 μg/L; Cr: 57 ± 13 μg/L; Hg: 0.28 ± 0.12 μg/L; and As: 2.6 ± 1.4 μg/L. In 2011, Karvelas and colleagues reported pertinent data on heavy metal concentrations in wastewater effluents from secondary sedimentation tanks, including Pb at 27 ± 3.6 μg/L, Cd at 1.5 ± 0.74 μg/L, Cr at 20 ± 3.5 μg/L, Zn at 270 ± 53 μg/L, and Ni at 430 ± 97 μg/L [5]. Agoro et al. 2020 [6] conducted research on the dispersion of five heavy metals (Cd, Pb, Cu, Zn, and Fe) in wastewater and sewage sludge within their waterbodies in the Eastern Cape Province, South Africa.

The presence of heavy metals in waterbodies and soils can lead to various health problems for both humans and ecosystems. Chromium, cadmium, and arsenic are classified as carcinogenic, while lead is designated as a potential carcinogenic metal by the International Agency for Research on Cancer (IARC) [7,8].

It is evident that the removal of heavy metals is crucial from wastewater effluents to reuse these effluents for irrigation or other uses. Several established technologies address this challenge, each with its unique strengths and weaknesses [9]. Activated carbon [10], biochar [11], and clay minerals [10] offer versatile and cost-effective options, but their effectiveness varies depending on the specific metal. Chemical precipitation and membrane technologies, such as reverse osmosis, excel in removal efficiency but can be energy-intensive or generate waste [12]. Biological approaches like biosorption are eco-friendly but slower and less widely applicable. Advanced oxidation processes like photocatalysis and the Fenton process boast broad contaminant removal but require careful handling and may have limited scalability [9,12].

Over the last two decades, iron nanoparticles have been investigated as promising agents for removing contaminants from soils, groundwater, and other sources [13-16]. Their high surface area allows for efficient adsorption and transformation of harmful metals into less toxic forms through reduction [17, 18]. Additionally, their potential for in-situ remediation offers exciting possibilities for direct water treatment [19]. However, the potential mobility and fate of iron nanoparticles should be considered for in-situ applications. To minimize risks, incorporating them into an inert porous matrix and using them as a water treatment filter is suggested.

In this study, an iron nanocomposite containing iron nanoparticles supported in a cationic resin (Amberlyst 15 H^+) was evaluated for cleaning up a polluted water stream containing heavy metals (Cr(VI), As, Ni, Pb, Cu, Cd, and Zn). Resin-supported nano-iron (R-nFe) is a nanocomposite material with high potential for remediating contaminated waters [20]. The resin can remove cationic metal contaminants through cation exchange or chelation processes, while nano zero-valent iron (nZVI) can also eliminate anionic contaminants, such as Cr(VI), by reducing it to Cr(III), or adsorb As(V) onto the oxidized outer shell of nZVI. The experimental work involved a series of column

tests with different contact times of the feed solution with the nanocomposites, namely 2.4, 4.8, and 6 minutes. To evaluate the potential use of effluents from a wastewater treatment plant (WWTP) as treated wastewater for various applications (e.g., irrigation, industrial use, or potable water), it was crucial to add it in the feed solution. The composition of the feed solution simulated the effluents of wastewater treatment plants contaminated with heavy metals, and the removal mechanisms were described in detail.

2 Materials and Methods

2.1 Synthesis of R-nFe

This study describes the synthesis of a resin-nZVI nanocomposite, R-nFe. Amberlyst 15 H^+ (Sigma-Aldrich, China), a macro reticular polystyrene based ion exchange resin with strongly acidic sulfonic groups, was used as the host matrix. Iron chloride ($FeCl_3 \cdot 6H_2O$) served as the iron source, and dry leaves of green tea (Twining of London) provided polyphenols. The detailed synthesis procedure is illustrated in Fig. 1.

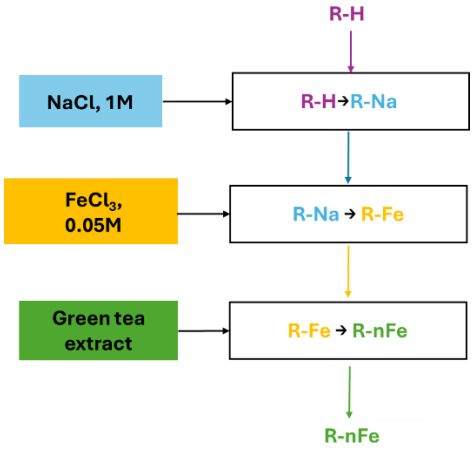

Fig. 1. The main steps of R-nFe synthesis procedure.

A pre-conditioning step to improve the reactivity of the resin-iron nanoparticle composite (R-nFe) towards pollutant capture was implemented. This involved stirring the R-nFe in a 1 M NaCl solution for 24 hours at 200 rpm with a 1:10 R-nFe -to-solution ratio. This NaCl pre-treatment enhances the reactivity of R-nFe with target pollutants, possibly due to the corrosion of nZVI particles [21]. The total iron content of R-nFe was determined to be 0.50 mmol/g, while the reactive elemental iron content, responsible for pollutant removal, was estimated at 0.35 mmol/g.

2.2 Column experiments

The performance of the R-nFe nanocomposite for pollutant removal was evaluated through column experiments conducted over a period of 12 days, with experiments

paused during weekends. Polyethylene columns with an internal diameter of 2.63 cm and a length of approximately 10 cm were employed. These columns were filled with varying amounts of the R-nFe nanocomposite: 12.5 g, 25.0 g, and 34.9 g, corresponding to volumes of 16.3 mL, 32.6 mL, and 43.5 mL, respectively. The nanocomposite was manually packed into the columns with gentle vibration at intervals to ensure homogenous packing. Table 1 provides detailed information regarding the properties of the three columns. The final bulk density in the columns, a measure of packing efficiency, ranged from 0.79 to 0.86 g cm^{-3} (as shown in Table 1). The packed columns were then connected to a pump and a reservoir containing the test solutions (Fig. 2). A schematic diagram of the experimental setup is presented in Figure 2.

Table 1. Properties of columns

	Columns		
Properties	**I**	**II**	**III**
Resin Mass weight, M ($kgx10^{-3}$)	12.50	25.00	34.9
Column diameter, d (cm)	2.63	2.63	2.63
Column height, L (cm)	3	6	8.0
Bed Volume, BV (cm^3)	16.3	32.6	43.5
Particle density, ρ_p (g/cm^3)	1.21	1.21	1.21
Bulk density, $\rho_b^{(a)}$ (g/cm^3)	0.77	0.77	0.80
Porosity, $\theta^{(b)}$	0.37	0.37	0.34
Pore volume, V_{PV} (cm^3)	6	12	14.47
Flow rate, Q (mL/min)	2.5	2.5	2.5
Pore Volume Contact Time, $\tau^{(c)}$ (min)	2.4	4.8	5.9
Empty Bed Contact Time, $EBCT^{(d)}$ (min)	6.5	13	17.3

(a) Dry bulk density calculated based on this equation $\rho_b=M/BV$
(b) Porosity calculated based on this equation $\theta=1-\rho_b/\rho_p$
(c) $\tau=Q/V_{PV}$
(c) EBCT=Q/BV

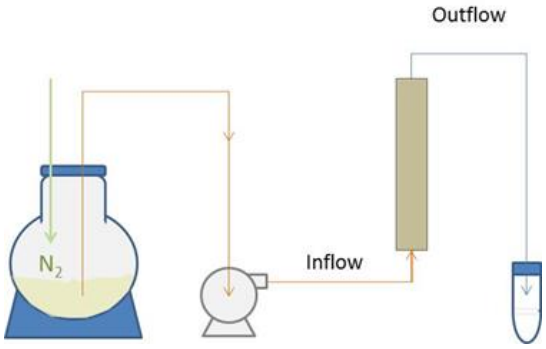

Fig. 2. Experimental set up [20]

The three columns were fed with a solution consisting of 44.4 mL/L Psyttalia WWTP effluents (2nd stage treatment) diluted with tap water of National Technical University of Athens (supplied by a drilling in the campus). The Psyttalia WWTP is the main wastewater treatment plant in Athens, Greece, receiving an average wastewater flow of approximately 730,000 m^3/d). The solution was also spiked with a concentrated solution of a mixture of heavy metals (5 mL/L) to obtain the predetermined level of metal contaminants, i.e. 500 μg L^{-1} Cr(VI), 2 mg L^{-1} Ni, 1 mg L^{-1} Pb, 2mg L^{-1} Cu, 100 μg L^{-1} Cd, 20 mg L^{-1} Zn and 2 mg L^{-1} As (Table 2). The metal concentrations in the feed solution were selected to be approximately ten times higher than the limits which were established by the Greek legislation for recycling the WWTP effluents in other uses [22]. The pH of the solution was adjusted to 3.5 using concentrated HCl. The flowrate was constantly 2.5 mL/min and was the same for the three columns. Taking into consideration the bed volume and the porosity of the 3 packed beds, the contact time of the solution with the R-nFe beads was 2.2 min, 4.8 min, and 5.9 min, in the shortest, middle and highest size bed, respectively. The main physicochemical properties of tap water (TW) and feed solution are presented in Table 2.

2.3 Sampling and analyses

Column effluents were sampled and analyzed for pH, EC and concentrations of hexavalent chromium, Cu, Cd, Zn, As, Ca, Mg. Cu, Ca, Mg and Zn concentrations were determined by atomic absorption spectroscopy-flame emission, AAS-FE. Cd concentrations were determined by graphite absorption spectroscopy-flame emission Hexavalent chromium was analyzed by using the USEPA 7196a method, at a HACH DR-1900 spectrophotometer. Arsenic concentrations were analyzed applying ASTM D5673:2016 method at EAGME laboratory. pH values were measured using a pH meter Metrohm 827 pH Lab. Ni and Pb will be analyzed by ICP-OES.

Table 2. Quality of tap water (TW) and feed solution.

Parameters	Units	Tap water (NTUA Campus)	Feed Solution	WWTP effluents reuse limits [22]
pH		7.3	3.5	
TOC	mg/L	8.6	2.6	
Alkalinity	mg $CaCO_3$/L	409	--	
Cr(VI)	μg/L	<15	500	
Ca	mg/L	106.1	116	
Mg	mg/L	36.2	24	
Na	mg/L	44.1		
K	mg/L	1.44		
Ni	mg/L	<0.2	2	0.2
Cu	mg/L	<0.1	2	0.2
Cd	mg/L	<0.04	0.1	0.01
Zn	mg/L	0.11	20	2
Pb	mg/L	<0.5	1	0.1
Cr	mg/L	<0.3		0.1
As	mg/L	<0.2	2	0.1

3 Results

3.1 Evolution of pH

Figure 3 shows the pH values in the effluent solutions as a function of the hours of operation. The pH of feed solution was adjusted at 3.5. As shown in Fig. 3 the solution was strongly acidified when passed through the R-nFe beads. During the operation with the contaminated solution the pH in the outlet increased slowly from 1.5 to 3.5 at the end of the experiment (Fig. 3). The decrease of pH values observed at 75 and 170 hours is due to the interruption of operation during the weekends, which caused the acidification of the solution remaining in contact with the R-nFe beads inside the columns.

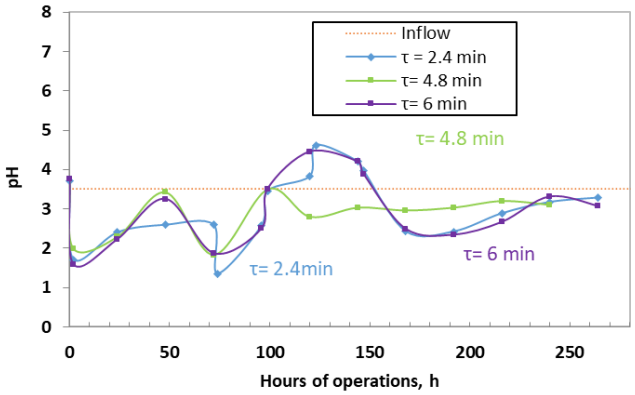

Fig. 3. Evolution of pH in the effluents of the three columns in comparison with the pH of inflow solution

3.2 Removal of Cr(VI)

The concentration of Cr(VI) in the feeding solution of columns was 500 μg/L. The effect of contact time on the Cr(VI) concentration in the effluent can be seen in Fig. 4. During the initial stages of operation, measurable amounts of Cr(VI) occurred after 50 hours of operation for column I (τ= 2.4min). The concentration of Cr(VI) in the effluents increased and reached a plateau at 325 μg/L, which is lower than the initial concentration of the feed solution. When the contact time of the polluted solution with the R-nFe was equal to 4.8 min (Column II), the Cr(VI) content in the effluent was constantly below detection limit for 74 hours of operation. Detectable values of Cr(VI), between 25 and 50 μg/L, appeared in the effluent for operation time from 74 to 144 hours. The concentration remained quasi constant, close to 200 μg/L, between 144 h and 264 h of operation. When the contact time of solution with R-nFe beads increased to 5.9 min (Col. III), all Cr(VI) was removed and the effluents did not contain any detectable amount for 216 hours. Measurable amounts of Cr(VI), from 50 to 185 μg/L, were observed after the 10^{th} day (240 h) of operation.

From the results shown in Figure 4, it can be estimated that a column filled with the nanocomposite R-nFe is able to reduce the concentration of Cr(VI) from 500 to less than 50 μg/L for a total amount of solution equivalent to 2400 bed volumes, if the contact time is at least equal to 5.9 minutes. The total volume is reduced to 1750 and 1250 bed volumes if the contact time is reduced to 4.8 and 2.4 minutes, respectively. It is seen however that the concentration of Cr(VI) in the effluent is lower than the inflow concentration even in the column with the lower contact time after 280 hours of operation.

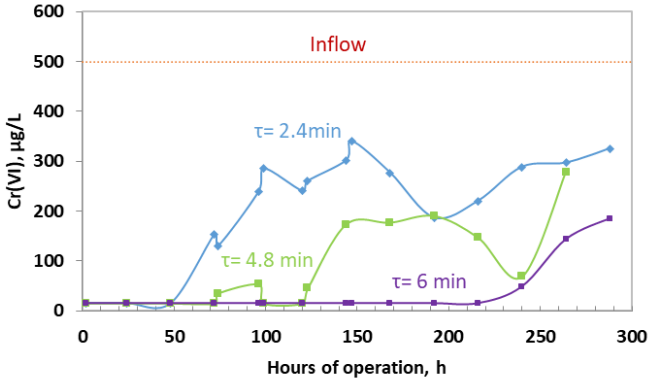

Fig. 4. Evolution of Cr(VI) concentration in the effluents of the three columns

The cumulative removal of Cr(VI) per gram of R-nFe, q_i, was calculated according to equation (2) and the corresponding curves are shown in Figure 5.

$$q_i = \frac{Q}{M_R} \sum_{1}^{i} (C_f - C_{e,i})\, \Delta t_i \tag{2}$$

where Q is the flowrate (ml/min), M_R is the mass of R-nFe in the column (g), C_f is the concentration of Cr(VI) in the feed solution (mg/mL), $C_{e,i}$ is the mean concentration of Cr(VI) in the effluents between the sampling events i-1 and i (mg/mL), and Δt_i is the time interval between sampling events i-1 and i (min).

In a previous publication by our team, the effectiveness of R-nFe for chromate removal was evaluated through batch experiments. All tests were conducted by mixing 100 mL of Cr(VI) solution with the appropriate amount of R-nFe in 250 mL shaking flasks. The experimental parameters examined included agitation rate, particle size of R-nFe beads, initial chromate concentration, nZVI content in resin, resin dose per liter of solution, and solution pH. Based on these batch tests, the maximum removal capacity of the nanocomposite was equal to 0.43 mmol Cr(VI)/g or 22.36 mg Cr(VI)/g [23]. It should be noted that the batch experiments in that study were carried out using deionized water, while in the present study the experiments took place using a more complex matrix containing competitive cations and anions. The results from that study are presented here for comparison with the current findings, which focus on chromate removal using a column study approach. As shown in Figure 5, it is evident that the maximum removal capacity was not exhausted, and the process is still in progress with a continuous increasing trend. The Cr(VI) removal after 288 hours of operation was equal to 1.0 mg/g, 6.3 mg/g and 5.7 mg/g for the columns with contact time 2.4, 4.8 and 6 min respectively.

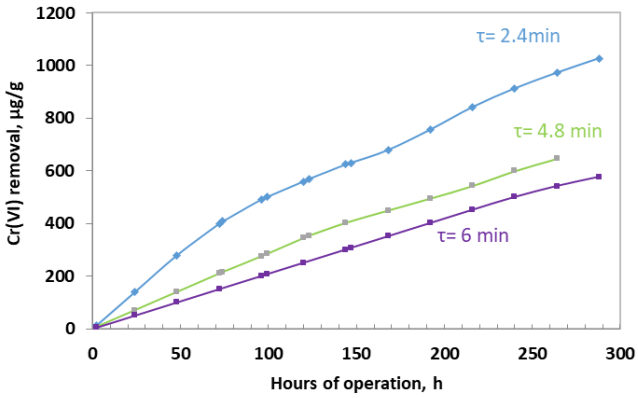

Fig. 5. Cumulative removal of Cr(VI) in the three columns

3.3 Removal of As

The evolution of arsenic in the effluent of the three columns is presented in Fig. 6a. High arsenic concentrations were detected in the 1st day of operation in Col. I and III. The arsenic concentrations decreased significantly after the 2nd day of operation in all three columns. Arsenic concentration in the effluents remained at low levels, <5-68 μg/L, till the end of experiment in Column III (τ=6 min). In Column II (τ=4.8 min), the concentrations were between <5 and 50 μg/L till 200 h and there was a slight increase above the limit of 100 μg/L at 264 h. The concentration of As in the effluents of Column I increased above the environmental limit after 150 h of operation.

The present work was carried out using pentavalent arsenic. As previously mentioned, the removal of arsenate using nZVI could be attributed to the precipitation of ferrous or ferric arsenates, such as $Fe_2(AsO_4)_3.8H_2O$ or $FeAsO_4.2H_2O$. However, the relatively low pH (3.5-4.5) excludes the precipitation of symplesite ($Fe_2(AsO_4)_3.8H_2O$). Symplesite is a compound with very low solubility (pKso=33.25) but precipitation starts above pH 5 and the minimum As concentration is observed at pH close to 8 [24]. Precipitation of scorodite $FeAsO_4.2H_2O$ occurs at acidic pHs but requires higher temperature conditions. During these experiments the most probable retention mechanism is chemisorption on the surface layer of Fe(III) oxides. A relative delay in the formation of oxidized surface layer around the nZVI particles could be the reason for the high concentrations of As observed in the first samples of effluents.

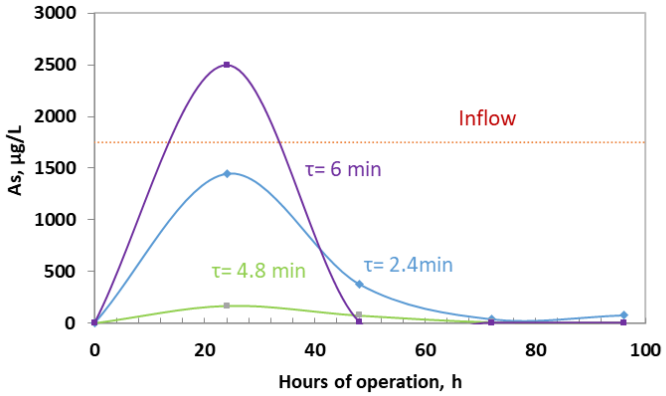

(a)

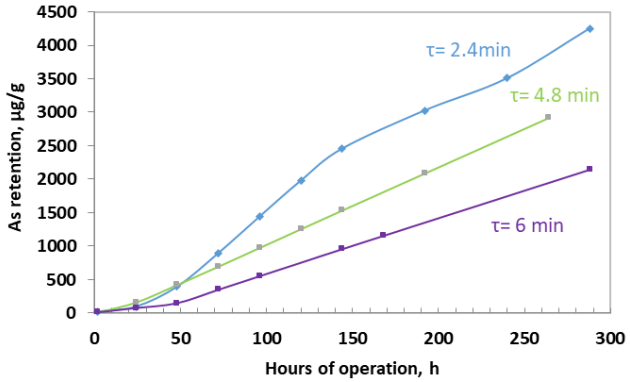

(b)

Fig. 6. Evolution of As removal in the 3 columns: (a) arsenic concentration in the effluents (µg/L), (b) cumulative retention in R-nFe (µg/g)

The cumulative retention of As by the R-nFe in the 3 columns is shown in Figure 6b. The retention increases almost linearly, indicating that the capacity of R-nFe to adsorb As is not exhausted. After 288 hours of operation the retention in column I (τ=2.4 min) is equal to 1026 µg/g.

3.4 Removal of divalent metal contaminants

The evolution of Cu concentration in the effluents of the 3 columns is shown in Figure 7a and the cumulative removal is shown in Figure 7b. As seen in Figure 7a, the concentration of copper in the effluents was maintained below the environmental limit 0.2 mg/L, only in column III (τ=6 min) and only for 24 hours of operation. This performance corresponds to the treatment of solution volume equivalent to 81.6 bed volumes.

In the other 2 columns with lower contact times Cu concentration exceeds the limit in the first sample taken at 24 hours.

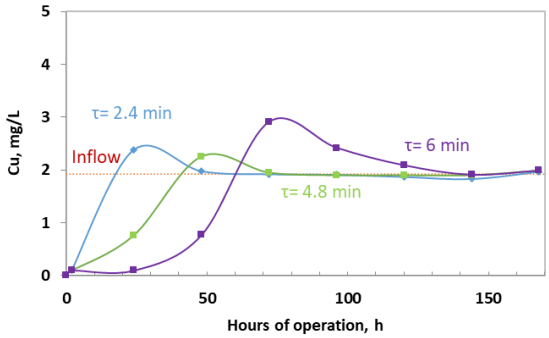

(a)

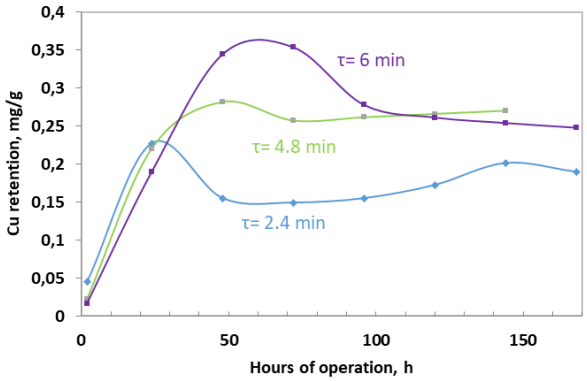

(b)

Fig. 7. Evolution of Cu removal in the 3 columns: (a) concentration in the effluents (mg/L), (b) cumulative retention in R-nFe (mg/g).

As shown in Figure 7b, the maximum cumulative retention of Cu by R-nFe in column III is equal to 0.35 mg/g, but there is a desorption effect, and the retention is finally stabilized close to 0.25 mg/g. A similar effect is observed in Column II (τ=4.8 min). In Column I (τ=2.4 min) the retention observe is lower in the order of 0.2 mg/g.

The results of Cd removal are shown in Figure 8. Concentrations below the limit of 10 μg/L were observed only in Column III and for the 24 initial hours of operation (Fig. 8a), similarly to the case of Cu. The final retention by R-nFe ranged between 14 and 18 μg/g (Fig. 8b).

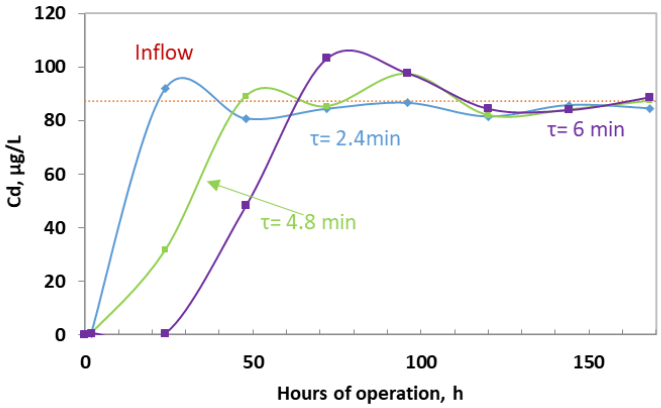

(a)

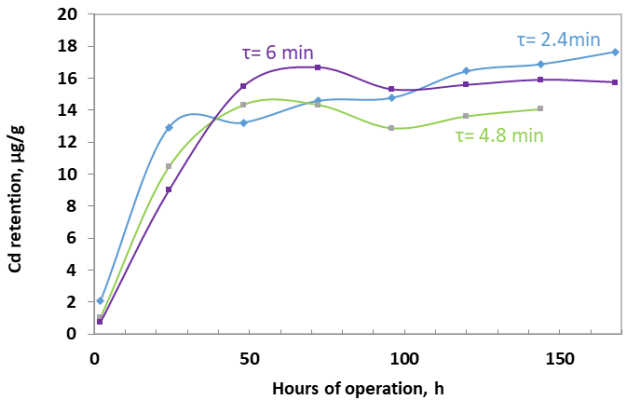

(b)

Fig. 8. Evolution of Cd removal in the 3 columns: (a) concentration in the effluents (µg/L), (b) cumulative retention in R-nFe (µg/g).

Zinc removal is presented at Figure 9. As previously observed a satisfactory performance was recorded only with column III (τ=6 min) for 24 hours (Fig. 9a). The appearance of a maximum value followed by a desorption effect was also very clear in the curves describing the cumulative retention of zinc by the R-nFe beads (Fig. 9b).

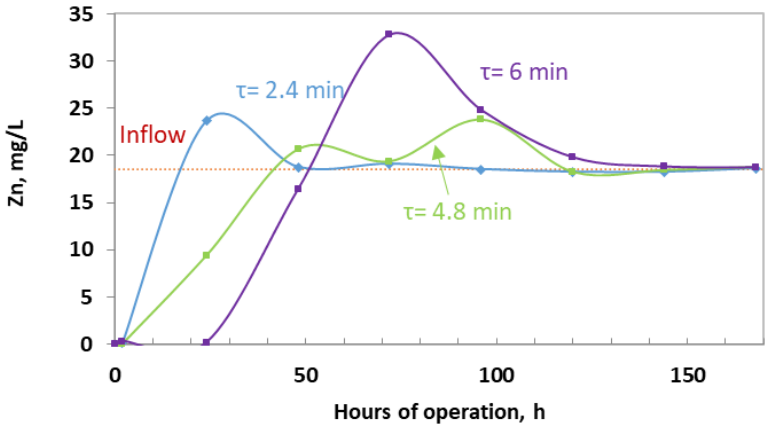

(a)

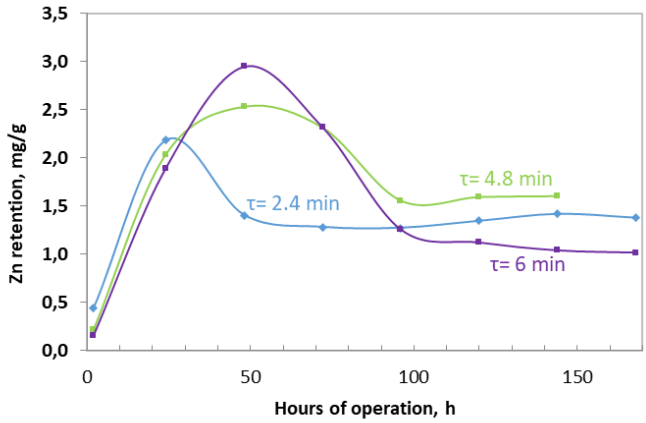

(b)

Fig. 9. Evolution of Zn removal in the 3 columns: (a) concentration in the effluents (mg/L), (b) cumulative retention in R-nFe (mg/g).

3.5 The effect of major divalent metals, Ca and Mg

The natural waters as well as WWTP effluents contain Ca and Mg at concentrations much higher than the concentration of usual metal contaminants (see Table 2). The water hardness is approximately 388.40 mg/L as $CaCO_3$ based on the calcium and magnesium concentration in the feed solution. To evaluate the effect of their presence, all the effluent solutions were also analyzed for these two metals. The results are presented in Figures 10 and 11 for Ca and Mg respectively.

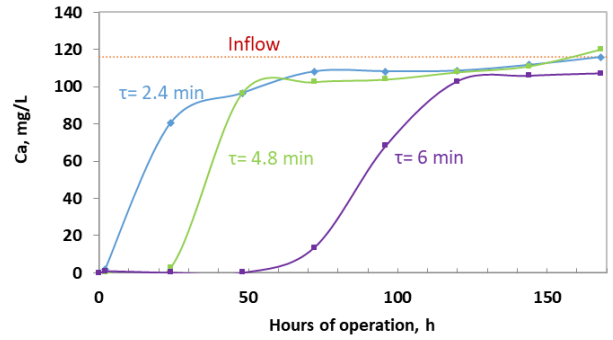

(a)

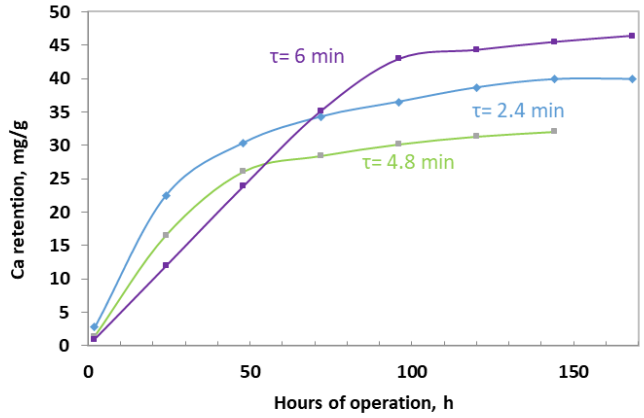

(b)

Fig. 10. Evolution of Ca removal in the 3 columns: (a) concentration in the effluents (mg/L), (b) cumulative retention in R-nFe (mg/g).

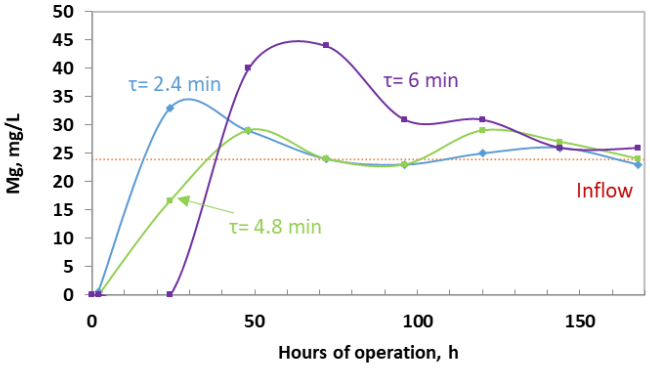

(a)

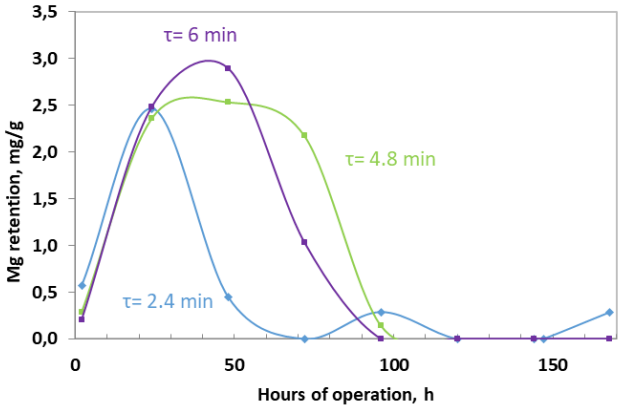

(b)

Fig. 11. Evolution of Mg removal in the 3 columns: (a) concentration in the effluents (mg/L), (b) cumulative retention in R-nFe (mg/g).

The breakthrough curves in Fig. 10a indicate that Ca is also retained by R-nFe. The concentration in the effluents approaches the value in the feed solution after 48 hours in Columns I and II and after 120 hours in Column III. The curves representing the cumulative retention of Ca follow a monotonic increasing trend, as seen in Figure 10b.

The removal of Mg follows a different trend. The charts in Figures 11a and 11b show that Mg is initially retained in the R-nFe, but after 72-96 hours of operation is completely repelled out of the resin beads.

The repulsion of Mg, as well as of other divalent metals, is obviously caused by the competitive adsorption of Ca. This is illustrated in Figure 12 for the case of Mg and Zn in the effluents of Column III in comparison with the levels of Ca. It is seen that all three elements are retained in R-nFe beads during the initial 24 hours. Between 24 and 96 hours, Ca continues to be retained and replaces Mg and Zn in the cation exchange

matrix of the resin. This effect can explain the fact that the concentrations of Zn and Mg in the effluents are higher compared to their concentration in the feed solution.

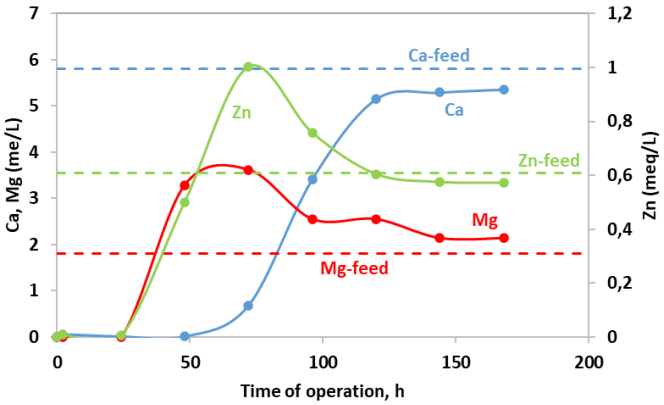

Fig. 12. The evolution of Mg, Zn and Ca concentration in the effluents of Column III.

3.6 Selectivity factors for the retention of divalent cations on the strongly acidic cation exchange resins

The host matrix of R-nFe material is a strongly acidic cation exchange resin with sulphonic functional groups. According to Amberlite and Dupont manufacturers this type of resins exhibits high selectivity of Ca towards most heavy metals. A typical selectivity scale is shown in Table 3.

Table 3. Typical selectivity scale of sulphonic resins for divalent metals

Mg^{++}	Zn^{++}	Co^{++}	Cu^{++}	Cd^{++}	Ni^{++}	Mn^{++}	**Ca^{++}**	Pb^{++}
0.63	0.67	0.71	0.73	0.75	0.75	0.79	1	1.9

The high affinity of the resin for Ca can explain the trend of breakthrough curves and the poor performance of R-nFe material for Zn, Cu, Ni and Cd removal from treated waters.

The total cation exchange capacity of the host matrix is equal to 2.7 meq/g. It calculated the milli-equivalents of divalent and trivalent cations retained in R-nFe after 168 hours of operation in the three columns. Due to the low pH (2.5-3.5), we have assumed that the reduced Cr(III) and the Fe(III) generated from the oxidation of nZVI do not precipitate but are simply retained electrostatically by the sulfonic groups. The percent distribution of retained metal equivalents is shown in Figure 13.

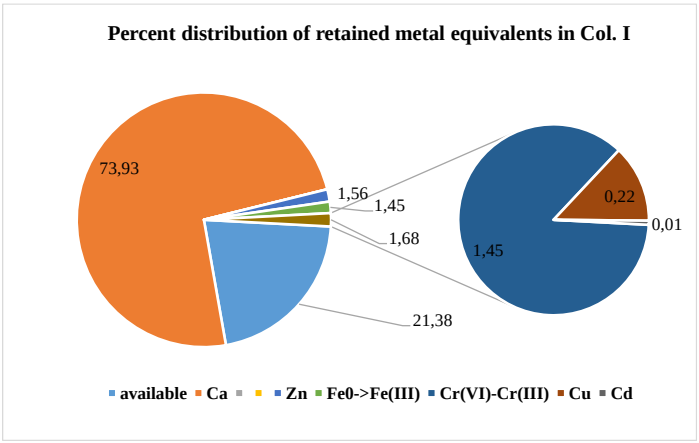

(a)

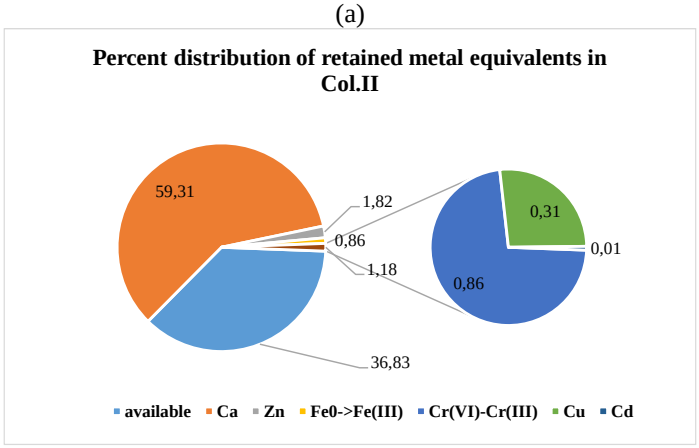

(b)

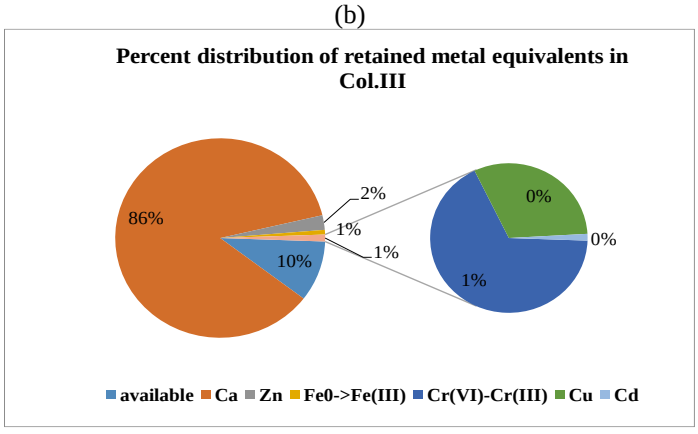

(c)

Fig. 13. Percent distribution of retained metal equivalents in the 3 columns after 168 hours for Columns I and III, and 144 hours of operation for Column II.

As seen in Fig. 13 a major part of cation exchange capacity is occupied by Ca cations, followed by Zn. Magnesium was completely expelled for all three columns.

4 Discussion

4.1 Mechanisms involved in the removal of metal contaminants by R-nFe

Nanocomposite R-nFe consists of elemental iron nanoparticles (nZVI) incorporated in a cation exchange resin. Both the host matrix and nZVI particles contribute in the removal of metals and a brief description of the mechanisms is given below.

Reactivity of nZVI

The reactivity of nZVI is primarily related with the strong reducing capacity of metallic iron. Data for selected redox reactions involving characteristic inorganic and organic contaminants are given in Table 4. Two columns with values of standard reduction potential are included in the table. The first corresponds to the standard potential, Eh^0, where proton activity is considered equal to one molar. The values in the second column, Eh^0 (pH=7), were calculated assuming pH equal to 7. This series of values is considered to be more representative of the conditions prevailing in natural waters. Data are presented in order of decreasing Eh^0 (pH=7). The reducing strength of the species to the left side of the reactions tends to increase towards the bottom of the Table. As seen elemental iron is situated very low in this order and theoretically can reduce all the oxidized species situated above, i.e. with higher Eh^0 (pH=7) values.

Table 4. Standard reduction potential for characteristic metal contaminants.

Half reactions	E_h^0 (V)	E_h^0 (pH=7)(V)
$Hg^{2+} + 2e^- \leftrightarrow Hg$	0.86	0.86
$Ag^+ + e^- \leftrightarrow Ag$	0.80	0.80
$CrO_4^{2-} + 8H^+ + 3e^- \leftrightarrow Cr^{3+} + 4H_2O$	1.51	0.41
$Cu^{2+} + 2e^- \leftrightarrow Cu$	0.34	0.34
$Pb^{2+} + 2e^- \leftrightarrow Pb$	-0.13	-0.13
$H_2AsO_4^- + 3H^+ + 2e^- \leftrightarrow H_3AsO_3 + 3H_2O$	0.42	-0.20
$Ni^{2+} + 2e^- \leftrightarrow Ni$	-0.25	-0.25
$Cd^{2+} + 2e^- \leftrightarrow Cd$	-0.40	-0.40
$Fe^{2+} + 2e^- \leftrightarrow Fe$	**-0.44**	**-0.44**
$Zn^{2+} + 2e^- \leftrightarrow Zn$	-0.76	-0.76
$Ba^{2+} + 2e^- \leftrightarrow Ba$	-2.92	-2.92

Among the metals presented in Table 4, Hg^{+2}, Ag^{+1}, Cu^{+2}, Pb^{+2}, Ni^{+2} and Cd^{+2} are cations which theoretically can be reduced by metallic iron to the elemental state. On

the contrary Zn^{2+} cannot be reduced because it is situated below iron in the reduction potential scale.

Hexavalent chromium, Cr(VI), exists in the form of anions, CrO_4^{2-}, and when reduced in the trivalent state under the action of elemental iron precipitates in the form of low solubility solid compounds, such as mixed Fe-Cr hydroxides as shown in equation (1):

$$Fe^0 + HCrO_4^- + 2H_2O + H^+ \rightarrow Fe(OH)_3Cr(OH)_3 + H^+ \quad (1)$$

Arsenic is a metalloid and its usual forms in aquatic media are the pentavalent and trivalent oxyanion species, $H_2AsO_4^-$ and H_3AsO_3. Pentavalent arsenic in the presence of Fe(II) and Fe(III) precipitates in the form of ferrous and ferric arsenate phases like symplesite, $Fe_3(AsO_4)_2 \cdot 8H_2O$ and scorodite, $FeAsO_4 \cdot 2H_2O$. Trivalent arsenic does not form any stable solid compound, but it is known to adsorb on the surface of iron oxyhydroxides.

When the metals have a redox potential more negative or close to that of iron, e.g. Zn, Cd, the preponderant removal mechanism is adsorption or co-precipitation with Fe(II) and Fe(III). It should be noticed that a second very important mechanism related with the reactivity of nZVI is due to its core-shell structure. When the metallic iron nanoparticles come in contact with the aquatic environment, their surface is oxidized and a layer of iron oxides is rapidly formed around the metallic core. The iron-oxides shell provides a very efficient substrate for the adsorption of contaminants.

Contribution of the cation-exchange resin

The matrix used for the incorporation of nZVI is a cation exchange resin. The cations retained in the resin after the synthesis procedure are primarily monovalent, e.g. H^+ or Na^+. It is known that during the cation exchange processes, cations with higher ionic charge are stronger bound to the resin and can replace cations with lower charge. It thus expected that divalent metals will be removed from the aqueous phase by replacing H^+ and Na+ in the resin. However, natural waters, as well as WWTP effluents, contain also alkaline earth metals such as Ca^{+2} and Mg^{+2}, which may compete with the metal contaminants in the cation exchange process.

5 Conclusions

This study focused on the effectiveness of a novel nanocomposite material, resin-supported nanoiron (R-nFe), for remediating water contaminated with heavy metals, including Cr(VI), As, Ni, Pb, Cu, Cd, and Zn. The experimental results revealed that the iron nanocomposite exhibited significant potential in removing Cr(VI) and As from the water stream. The column experiments demonstrated varying degrees of efficiency depending on the contact time between the feed solution and the nanocomposite. Particularly noteworthy was the efficient removal of Cr(VI) from the water, with concentrations dropping to less than 50 μg/L when the contact time is 6min. The study also highlighted the dynamic interactions between R-nFe and various heavy metals, elucidating mechanisms involving reduction, adsorption, and cation exchange facilitated by

the resin matrix. Additionally, the research shed light on the intricate competition between divalent metals, such as Ca and Mg, and the targeted contaminants during the cation exchange process within the resin-supported nanocomposite. Overall, the findings underscore the promising potential of R-nFe for water treatment applications, offering insights into its mechanisms and selectivity factors critical for future advancements in water remediation technologies.

References

1. World Bank Group, UNICEF. State of the World's Drinking Water report (2022).
2. WWAP. The United Nations World Water Development Report 2023: Water Security for Humanity. UNESCO Publishing (2023).
3. UN DESA. World Population Prospects 2022. United Nations Department of Economic and Social Affairs (2022).
4. Du, P., Zhang, L., Ma, Y., Li, X., Wang, Z., Mao, K., Wang, N., Li, Y., He, J. Zhang, X. Occurrence and Fate of Heavy Metals in Municipal Wastewater in Heilongjiang Province, China: A Monthly Reconnaissance from 2015 to 2017. Water 12, 728 (2020).
5. Karvelas, M., Katsoyiannis, A., Samara C. Occurrence and fate of heavy metals in the wastewater treatment process. Chemosphere, 53 1201–1210 (2003).
6. Agoro, M.A., Adeniji, A.O., Adefisoye, M.A. and Okoh, O.O. Heavy Metals in Wastewater and Sewage Sludge from Selected Municipal Treatment Plants in Eastern Cape Province, South Africa. Water, 12, 2746 (2020).
7. EPA. Volume I: Human Health Evaluation Manual (Part a) Washington, DC, USA: EPA. Risk assessment guidance for superfund (2004).
8. IARC. IARC Monographs on the Identification of Carcinogenic Hazards to Humans: Volumes 1–125. Bristol, UK: IOP Publishing PhysicsWeb (2012).
9. Hashim, M.A., Mukhopadhyay, S., Sahu J. N., Sengupta, B. Remediation technologies for heavy metal contaminated groundwater, Journal of Environmental Management, 92, 10, 2355-2388 (2011).
10. Karnib, M., Kabbani, A., Holail, H. and Olama, Z. Heavy Metals Removal Using Activated Carbon, Silica and Silica Activated Carbon Composite, Energy Procedia, 50, 113-120 (2014).
11. Wang, Y., Li, H., Lin, S. Advances in the Study of Heavy Metal Adsorption from Water and Soil by Modified Biochar. Water, 14, 3894 (2022).
12. Qasem, N. A. A., Mohammed, R. H. D. U. and Lawal D.U. Removal of heavy metal ions from wastewater: a comprehensive and critical review npj Clean Water 4, 36 (2021).
13. Dave, P.N. and Chopda, L. V. Application of Iron Oxide Nanomaterials for the Removal of Heavy Metals. Journal of Nanotechnology. 398569, 14 p. (2014). http://dx.doi.org/10.1155/2014/398569.
14. Vijaya Bhaskar Reddy, A., Moniruzzaman, M., Madhavi, G. Removal of Heavy Metal Pollutants from Wastewater Using Zerovalent Iron Nanoparticles. Water Pollution and Remediation: Heavy Metals. Environmental Chemistry for a Sustainable World, 53 (2021).
15. Mohamed, A., Atta, R.R., Kotp, A.A. Green synthesis and characterization of iron oxide nanoparticles for the removal of heavy metals (Cd^{2+} and Ni^{2+}) from aqueous solutions with Antimicrobial Investigation. Scientific Reports 13, 7227 (2023).

16. Xu, W., Yang, T., Liu, S., Du, L., Chen, Q., Li, X., Dong, J., Zhang, Z., Lu, S., Gong, Y., Zhou, L. Liu, Y., Tan, X. Insights into the Synthesis, types and application of iron Nanoparticles: The overlooked significance of environmental effects, Environment International, 58, 106980 (2022).
17. Dermatas, D., Mpouras, T., Papassiopi, N., Mystrioti, C., Toli, A. and Panagiotakis, I. Adsorption of Groundwater Pollutants by Iron Nanomaterials. Iron Nanomaterials for Water and Soil Treatment. 1st edn. Jenny Stanford Publishing (2018).
18. Tarekegn, M. M., Hiruy, A. M. and Dekebo, A. H. Nano zero valent iron (nZVI) particles for the removal of heavy metals (Cd^{2+}, Cu^{2+} and Pb^{2+}) from aqueous solutions. RSC Advances, 11, 18539 (2021).
19. Mondal, A., Dubey, B. K., Arora, M. and Mumford, K. Porous media transport of iron nanoparticles for site remediation application: A review of lab scale column study, transport modelling and field-scale application, Journal of Hazardous Materials, 403, 123443, (2021).
20. Toli, A., Mystrioti, C., Avgoustidis, I., Papassiopi, N., Fixed-bed flow experiments with supported green nZVI for the remediation of contaminated waters: Effect of pH and background solution composition, Chemosphere, 279, 130472 (2021).
21. Panagou, I., Noutsopoulos, C., Mystrioti, C., Barka, E., Koumaki, E., Kalli, M., Malamis, S., Papassiopi, N., Mamais, D. Assessing the Performance of Environmentally Friendly-Produced Zerovalent Iron Nanoparticles to Remove Pharmaceuticals from Water. Sustainability, 13, 12708 (2021).
22. Common Ministerial Decision No. 145116, 2011 (FEK 354/B/2011).
23. Toli, A., Varouxaki, A., Mystrioti, C., Xenidis, A. and Papassiopi N. Green Synthesis of Resin Supported Nanoiron and Evaluation of Efficiency for the Remediation of Cr(VI) Contaminated Groundwater by Batch Tests. Bulletin of Environmental Contamination and Toxicology 101:711–717 (2018).
24. Johnston, R. and Singer, P. Solubility of Symplesite (Ferrous Arsenate): Implications for Reduced Groundwaters and Other Geochemical Environments. Soil Sci. Soc. Am. J. 71:101-107 (2007).